POTASSIUM TERBIUM FLUORIDE CRYSTAL
GROWTH DEVELOPMENT FOR FARADAY
ROTATOR DISCS FABRICATION

6 JULY 78 - 6 FEBRUARY 79

P.O. 1391009

SA ⚠ **SANDERS**
ASSOCIATES, INC.

DEFENSIVE SYSTEMS DIVISION

95 Canal Street
Nashua, New Hampshire 03060

MAY 17, 1979

PREPARED FOR:

UNIVERSITY OF CALIFORNIA
LAWRENCE LIVERMORE LABORATORY
P.O. BOX 5012
LIVERMORE, CALIFORNIA   94550

TABLE OF CONTENTS

LIST OF FIGURES

ABSTRACT

Crystal growth experiments were performed and growth of KTb_3F_{10} crystals were accomplished. The crystal growth experiments consisted of hot zone modification and development of growth parameters. Several boules of KTb_3F_{10} 30-40mm in diameter and one boule 50mm in diameter were grown at rates varying from .5mm/hr to 3.0mm/hr.

The crystals evaluated display excellent optical quality. The optical path distortion was less than 0.5 fringe/cm at 633nm as viewed in Twyman-Green interferometry. Growth of large crystals has been limited by mechanical cleavage.

PREFACE

This report is an investigation of crystal growth
of potassium terbium fluoride material intended for application
to laser fusion as faraday rotator material. The investigation
was funded by the University of California, Lawrence Livermore
Laboratory. The period covered in this report was 6 July 1978
to 6 February 1979.

Dr. Marvin Weber of the Lawrence Livermore Laboratory,
University of California was program monitor of this study.

This study was performed by the Energy Systems Center,
Defensive Systems Division of Sanders Associates, Inc.
Mr. Robert C. Folweiler was Principal Investigator at Sanders.
Mr. Folweiler was directly assisted by Mr. Thomas M. Pollak
in the design and evaluation of crystal growth experiments.
Mr. James Mosto assisted in the hot zone design for the
crystal furnace. The crystal growth of KTb_3F_{10} and sample
fabrication tasks at Sanders were done by P. Foley and L.
Terrenzio.

1.0 SUMMARY

1.1 Introduction

The objective of this program was to grow KTb_3F_{10} crystals and fabricate them for application as Faraday rotator discs to be used in laser amplifier chains. The specific goals of this program include:

Growth and fabrication of two KTb_3F_{10} discs
7.0 cm x 1.0 cm

Growth of samples for hot forging experiments.

The contract was conducted by Sanders Associates at its Merrimack, New Hampshire facility.

1.2 Background

Sanders crystal growth facility has been involved with the development of crystalline fluoride material with emphasis on the laser host, $LiYF_4$ (YLF) for over six years. The crystal growth facility centers around the automated control furnace (Figure 1) in which all crystal growth experiments for this program were carried out. The existing hot zone was designed to grow 30mm YLF crystals. Monitor and control of the growing crystal is performed by a unique electro-optical system in which a laser beam is employed to "observe" the growth and produce an input signal for the computerized controller. This system provides a continuously looping control.

At the onset of this program, limited crystal growth development of KTb_3F_{10} had been accomplished. Boules about
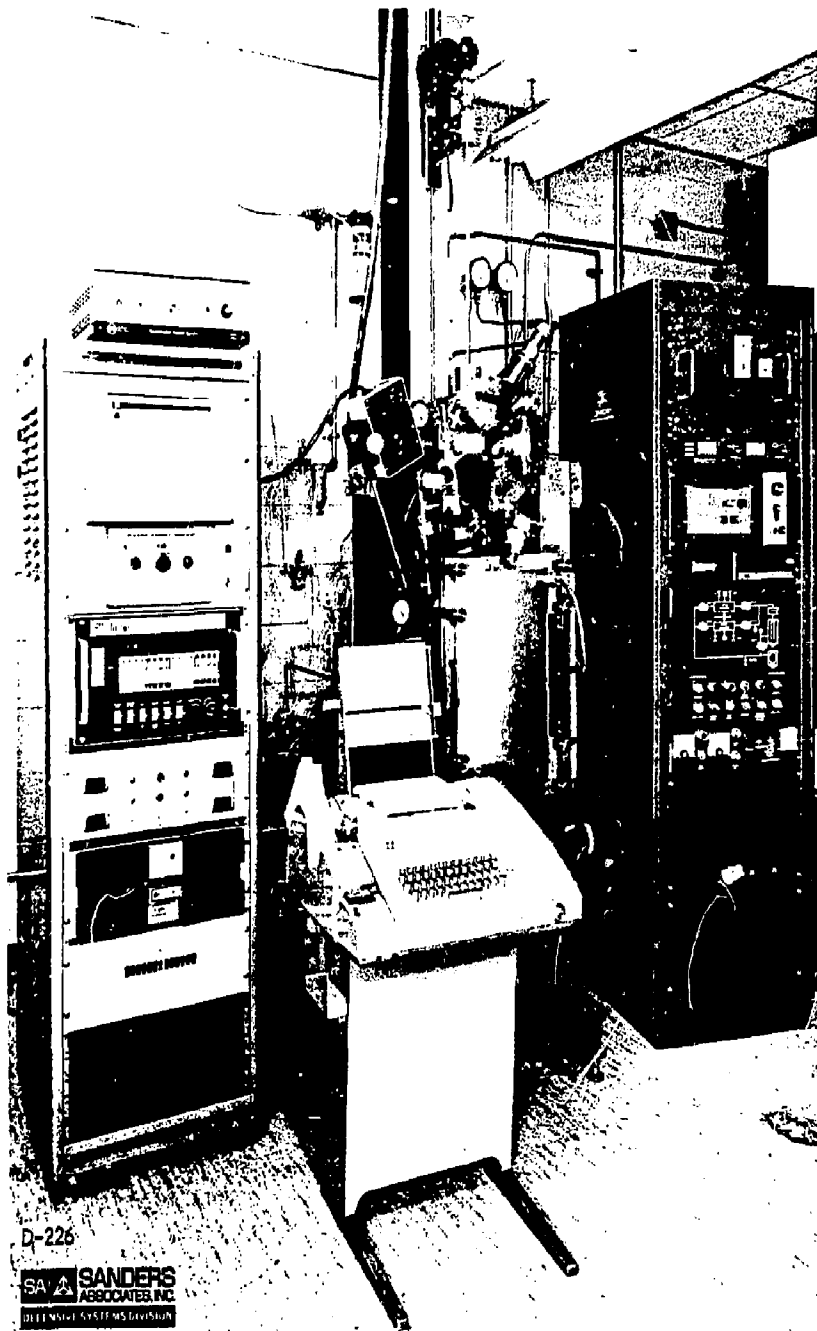
1

FIGURE 1

SANDERS AUTOMATED GROWTH FACILITY

10mm in diameter had been grown at the Crystal Physics
Laboratory M.I.T.[*] and were used to develop initial phase
diagram data. The magneto-optical properties of the
material[**] were evaluated at Lawrence Livermore Laboratories.
Experimental results showed that KTb_3F_{10} possessed one of the
highest figures of merit of all the known rotator materials.
The high verdet constant of this material together with its
cubic structure and low N_2 were the motivating factors in
this attempt to scale the growth for high power laser systems.

The state-of-the-art of crystal growth of KTb_3F_{10} prior
to this program can be summarized by the following:

- The nature of the existance of KTb_3F_{10} was not
  completely identified, i.e., compound or solid
  solution.

- Very little phase diagram data was available to
  describe the crystallization behavior of KTb_3F_{10}.

- Crystal growth was restricted to bᵤ ules about 10mm
  in size, as such material evaluation fabricated
  by Top Seeded Solution Techniques has been limited.

- Minimal development of growth parameters have
  occurred.

Despite the limited development of the growth of
KTb_3F_{10}, a program of growth scaling was initiated due
to the outstanding potential in laser fusion as Faraday
rotator material.

3

1.3 Results

A series of fifteen furnace experiments and crystal
growth runs were completed to develop a growth process for
KTb_3F_{10}. Highlights of the present program are summarized
below:

- KTb_3F_{10} was identified to exist as a solid
  solution, composition range 25 mole % KF
  to 40 or 50 mole % KF. Stoichiometic
  KTb_3F_{10} decomposes incongruently. [***]

- The hot zone of the Sanders' crystal furnace
  was modified to grow KTb_3F_{10} crystals up to
  70mm diameter.

- KTb_3F_{10} growth parameters were experimentally
  investigated and optimized, including seed
  rod rotation rate and growth rates.

- Several boules of KTb_3F_{10} were grown, up to
  50mm in diameter.

- Optical evaluation of a KTb_3F_{10} sample grown
  for this program displayed 0.5 fringe/cm
  of optical path distortion when viewed in
  Twyman-Green interferometry at 633nm.

- Scaled growth limitations at this time involves
  cleavage of KTb_3F_{10}. Probably thermal gradient
  driven, cleavage may be prevented by further
  shielding the upper chamber and proper seed
  orientation.

1.4 Future Work

- Proper seed orientation should be determined to eliminate cleavage. We anticipate that use of seeds oriented in the (100) direction is expected to control this problem, but further experimentation is required.

- The phase equilbria studies should be continued to better understand the $KF \cdot TbF_3$ system.

- Continued growth studies are necessary to determine the specific driving force causing the cleavage in growing crystals of KTb_3F_{10}. Work is presently being done on the analogous compound KT_3F_{10} and valuable information will be learned.

- Samples of KY_3F_{10} will be supplied for hot forging experiments, which should be followed by experiments on KTb_3F_{10}.
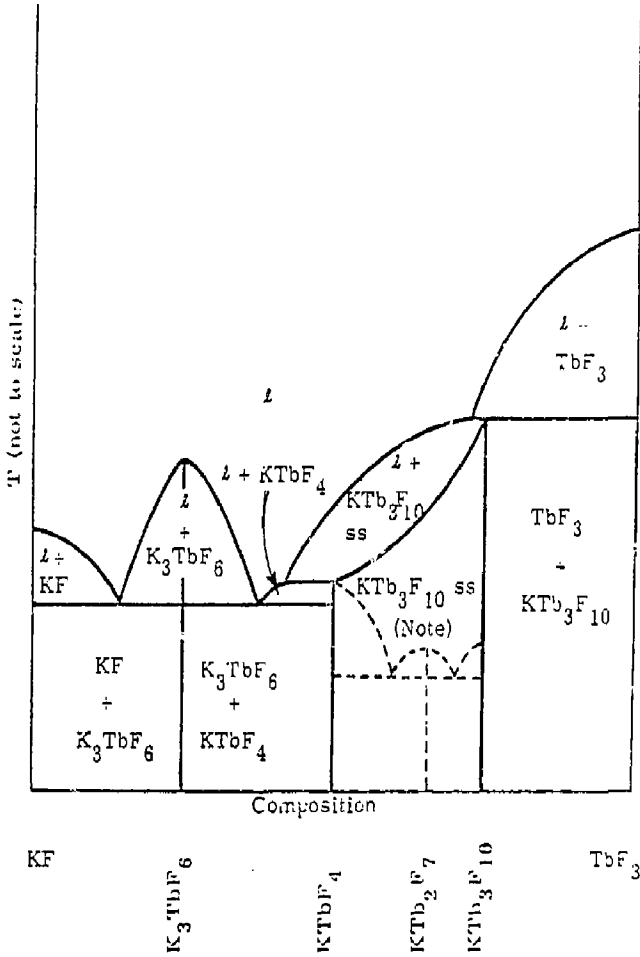
2.0 REVIEW

A critical optical component in the amplifier chain for the laser fusion program is the Faraday rotator. The Faraday rotator prevents the laser energy in the cavity from propagating in the reverse direction and potentially damaging a smaller, lower power element. Materials containing ions such as Tb^{+3} have a high specific unit rotary power within a magnetic field, termed the Verdet constant.[1]

For a specified rotation angle, a large Verdét constant will minimize the required magnetic field and/or linear optical path the energy must travel. It is, therefore, desirable to maximize the concentration of Tb^{+3} per unit of volume. In addition to a large Verdét constant, it is desirable for a rotator material used in high power laser applications to display properties such as small absorption and scattering losses, and small refractive-index nonlinearity. KTb_3F_{10} combines all these qualities and displays excellent potential for Faraday rotators.[2]

KTb_3F_{10} has a face centered cubic structure [3] and appears applicable to hot forging techniques that can be used to increase the diameter to thickness aspect ratio.

Preliminary studies on the $KF-TbF_3$ phase equilibria have yielded significant results.[4] It suggests that KTb_3F_{10} exists as a solid solution in the range of potassium fluoride concentration of 25 to 50 mole percent, as illustrated in Figure 2. In the system $KF-YF_3$, KY_3F_{10} exists to a concentration of 50 mole percent KF, the KTb_3F_{10} phase is expected to behave similarly. It has been demonstrated, however, that at a minimum composition of 35 mole percent potassium fluoride, decomposition of the KTb_3F_{10} phase readily occurs at lower temperatures. The decomposition reaction has been kinetically prevented by rapid quenching of the sample. A peritectic

6

T (not to scale)

ℓ

$\ell + KTbF_4$

$\ell +$ KTbF_{10} ss

$\ell +$ TbF$_3$

$\ell +$
KF

ℓ
+
K$_3$TbF$_6$

TbF$_3$

KTb$_3$F$_{10}$ ss
(Note)

TbF$_3$
+
KTb$_3$F$_{10}$

KF
+
K$_3$TbF$_6$

K$_3$TbF$_6$
+
KTbF$_4$

Composition

KF   K$_3$TbF$_6$ KTbF$_4$ KTb$_2$F$_7$ KTb$_3$F$_{10}$ TbF$_3$

Note: Only one possible subsolidus scheme is shown for the
crystallization behavior of the KTb$_3$F$_{10}$ solid
solution.

FIGURE 2

POTENTIAL PHASE DIAGRAM FOR THE SYSTEM KF-TbF$_3$

7

reaction occurs at a melt composition of 27 mole percent
potassium fluoride at which KTb_3F_{10} will decompose to TbF_3
and a KF enriched liquid.

The details of the subsolidus behavior of KTb_3F_{10}
has not been defined clearly to date. It is evident,
however, that KTb_3F_{10}, composition close to the peritectic,
will not undergo a phase change to a low temperature form.
Prolonged annealing experiments of KF lean KTb_3F_{10} has
produced only small amounts of a second phase percipitate.

3.0 CRYSTAL GROWTH OF KTb$_3$F$_{10}$

Crystal growth experiments and growth of KTb$_3$F$_{10}$ boules were performed in Sanders automated crystal growth furnace. This system employs a minicomputer for supervising and control. Feedback to the computer is supplied by optically sensing the diameter of the crystal, thus providing a signal to close the loop. Long term, continuous operation is permitted with minimum operator attention.

The furnace consists of stainless steel high vacuum construction to minimize contamination from the furnace walls. The hot zone consists of a graphite resistance heater enclosed in a series of insulating molybdenum heat shields. A high purity atmosphere is created by pumping the system to a vacuum of less than 30 μPa and backfilling with high purity argon to a pressure of 140 kPa.

The melt is typical processed in Sanders' hydro-fluorination system prior to entering the crystal growth furnace. The hydrofluorination system consists of a platinum lined ceramic tube, sealed at each end with Teflon caps, situated in a Kanthal coil heated furnace. The feed is usually purchased as either the oxide or carbonate powder and converted to the fluoride at a temperature below the melting point, using flowing HF. The converted fluoride powder is then melted under flowing HF in the cycle to complete conversion and reduce the surface area and volume.

3.1 Material Preparation for Crystal Growth

3.1.1 Powders

KTb$_3$F$_{10}$ used for the melts in this program were processed through Sander's fluoride conversion system as the raw materials were not purchased as fluorides. Tb$_4$O$_7$, 99.9%

pure, was purchased from Apache Chemicals (Table I summarizes the impurities). ULTREX grade, K_2CO_3 was supplied by J.T. Baker Company (Table 2). The terbium oxide was converted to TbF_3 in the hydro-fluorination system prior to mixing with K_2CO_3. The percent conversion was monitored by weight change of the material. TbF_3 and K_2CO_3 were mixed in specified ratios and processed for the final fluoride conversion. KF was not added directly as this material displays deliquescent tendencies. Again, total conversion was determined by material weight change.

3.1.2 Atmosphere

Hydrogen fluoride supplied by Matheson gas at a minimum purity of 99.9% was used in Sander's fluorination system. Titanium gettered argon was used to flush the fluorination system at the beginning and at the end of each cycle. Welding grade argon, typically containing 10 ppm oxygen was purchased and scrubbed in a titanium getter to reduce the measured oxygen concentration to a maximum of 10^{-10} ppm. The titanium getter system was improved later in the program, under contract with the Department of Energy, and decreased the oxygen contamination level to 10^{-16} ppm.

The argon used in the Sander's fluoride furnace in the early portion of this program was supplied by Airco. Initial purity level was a maximum of 1 ppm. Later in the program, the argon was processed to a purity level of 10^{-16} ppm of oxygen using the system mentioned above. The oxygen content of the furnace atmosphere was monitored by an oxygen sensor.

3.1.3 Process Improvements

Process improvements were made during the period of this program to reduce and eventually eliminate surface impurities on the melt. Surface examination of sample melts by Auger Spectroscopy, sponsored by the Department of Energy, identified

10

<div align="center">

TABLE 1

MASS SPECTROGRAPHIC ANALYSIS OF Tb_4O_7

</div>

ELEMENT		CONCENTRATION (ppm)
NITROGEN	-	50
SODIUM	-	190
SILICON	-	460
SULFER	-	180
CHLORINE	-	270
POTASSIUM	-	150
CALCIUM	-	500
IRON	-	80
RARE EARTH ELEMENTS		
NEODYMIUM	-	20
SAMARIUM	-	70
GADOLINIUM	-	300
DYSPROSIUM	-	1000
HOLMIUM	-	100
ERBIUM	-	90
THULIUM	-	15

NOTE: (1) Only major elements are listed.

  (2) Concentration estimates given are expected
       to be within a factor of three of the true
       concentration.

<div align="center">

11

</div>

TABLE 2

POTASSIUM CARBONATE, ULTREX

For Application in Fiber Optics Manufacture

COMMODITY NO. 5157
LOT NUMBER: 512561
DATE OF ANALYSIS: 5/2/75
DATE PACKAGED: 8/14/78

FORMULA: K_2CO_3
FW: 138.21

	ACTUAL ANALYSIS
ASSAY (K_2CO_3)(by acid-base titration, after drying at 285°C for 4 hours)	100.00 %[a]
Loss on drying at 285°C for 4 hours	0.40 %
Particulate matter (after solution in water)	0.001%

NON-METALLIC IMPURITIES
   In parts per million (ppm)

ARSENIC (As)[b]	0.04
HALIDES (as Cl)	3
Nitrogen Compounds (as N)	6
Phosphate (PO_4)	3
Sulfer Compounds (as SO_4)[c]	1

TRANSITION ELEMENTS[d]
   In parts per million (ppm)

CHROMIUM (Cr)	0.01
COBALT (Co)	0.01
COPPER (Cu)	0.01
IRON	0.1
MANEANESE (Mn)[e]	0.02
NICKEL (Ni)	0.02
VANADIUM (V)	0.01

a - Based on 3 determinations: 99.99%, 99.99%, and 100.02%

b - By evolution and silver diethyldithiocarbamate photometry.

c - By barium sulfate turbidimetry in methanol-water.

d - Average values for duplicate samples analyzed by
   dc-arc spectrography (after collection via coprecipitation
   with indium using 8-quinolinol-tannic acid-thionalide and
   ignition to oxides against commercial standards in indium
   oxide, reading of lines in 2450-3875 A region); key
   elements found at or below a significant blank value are
   reported as < (equal to or less than) one-third of the
   blank, key elements found at or below a blank near the
   detection limit are reported as < (less than) the
   detection limit, the blank values found have been deducted
   in all of the reported values.

e - By atomic absorption spectrophotometry.

the contaminants primarily as a mixture of carbon and oxides.
Carbon contamination probably occurs during the hydrofluorina-
tion process, in which the reaction by-product, steam, attacks
the graphite sagger. Rare earth oxides react with hydrogen
fluoride in the following manner:

$$RE_2O_3 + 6 HF \longrightarrow ReF_3 + 3 H_2O$$

The by-product water, or steam at the reaction temperature,
tends to attack graphite. Presently, a graphite sagger is
used to support the platinum boat. A thin layer of pyrolytic
graphite which acts as a kinetic barrier, has been deposited
on the graphite saggers to prevent the attack. The oxygen
getter and monitoring system was improved to reduce oxygen
to 10^{-16} ppm in the period of this program to reduce the
oxide impurity level.

3.2 Crystal Growth

The pertinent parameter variations and results are
summarized in Table 3. It was apparent early in the program
that the existing hot zone configuration of the Sander's
furnace was not applicable for growth of KTb_3F_{10}. The thermal
properties of KTb_3F_{10}, specifically radiation effects, differed
greatly from $LiYF_4$. The initial six growth runs were
specifically geared to modify the hot zone to optimize the
thermal distribution and enhance the radial thermal gradient.
In growth runs seven through ten, although minor modifications
were made to adjust the thermal balance, were concerned with
determining proper melt composition and optimizing growth parameters.
A polycrystalline boule (#546) of fair quality was grown in run
ten. In growth runs ten through fifteen, the 1-liter crucible,
supplied by the Department of Energy, was employed. The last five
runs were seeded with KTb_3F_{10} and growth parameters were altered to

GROWTH RUN	PARAMETER VARIATIONS	EVALUATION AND RESULTS
I	The position of the crucible in the hot zone and the design of the top horizontal heat shields were evaluated. The melt was seeded with platinum wire.	Observation of the convection flow in the melt indicated that a variation in the heat shield configuration had a significant effect on the thermal distribution of the melt.
II	The thickness of the platinum wire seed was increased to enhance the cooling effect of the seed rod.	The cooling effect of the seed rod was not changed significantly.
	The rotation speed of the seed rod was altered to change the interfacial shape of the boule.	Rotation speed was reduced from 40 rpm to 6 rpm, the crystal interface was altered from concave to flat in respect to the melt.
III	Fabricated and employed a 3 mm diameter molybdenum "seed" to replace the platinum wire seed (Fig. 3)	The thermal transport through the seed rod was increased, the initial growth temperature increased 10^0-15^0C. The molybdenum seed was mechanically more stable than the platinum seed.
	A cylindrical heat shield was developed to go over the seed rod.	No change in the thermal distribution was observed.
	The vertical concentric heat shields around the crucible was reduced from 4 to 2 layers. Less shielding would increase the percentage of radiative heat, as opposed to convective heating.	No evaluation was made.
IV	The top horizontal shield was modified from 2" to a 4" opening to allow heat to escape vertically.	The rate of nucleation of surface crystals at the crucible wall during the growth process was reduced. This indicates that the thermal gradient across the melt surface was increased.
		A small boule was pulled from the melt. The material appeared hazy.

14

GROWTH RUN	PARAMETER VARIATIONS	EVALUATION AND RESULTS
V	The vertical concentric shields around the crucible was shortened to 20 mm to increase the direct radiative heating.	Evaluation was difficult, a definite increase in measured growing temperature was recorded, indicating a larger thermal gradient; however, the growth was composed of a non-cubic, higher melting temperature phase. The relative importance of each effect on the measured temperature is not known.
	The crucible was positioned in the upper level of the hot zone. The crucible was thus heated from the sides and bottom.	The result of the change was a colder surface, more applicable for seeding and growth. The effects were observed as frequent nucleation of crystals on surface impurities and crucible wall.
VI	The crucible was lowered to the middle section of the hot zone to increase the direct heating of the upper section of the crucible.	The heat distribution was altered considerably, observed by the increase in the stability of the melt surface; the lack of surface crystal nucleation. The cooling effect of the seed was hampered, due to the direct radiation to which the seed rod was subjected.
VII	The heat shield configuration and crucible position developed in Run V were employed. All impurities were removed from the surface of the melt.	The removal of surface impurities resulted in a cooler yet stable surface, which facilitated nucleation on the seed.
VIII	Identical parameters were employed; material was pulled from the melt to "grow" into the cubic, KTb_3F_{10}, phase. melt composition was initially 26% KF.	Petrographic analysis indicated TbF_3 was present rather than KTb_3F_{10}. The melt was depleted of KF.
IX	The melt was thermally cycled to observe convection flow and empirically adjust the thermal distribution of the melt.	Observation of the pattern of floating particles facilitated the exercise. Adjustments were made to the position and level of the crucible to optimize the thermal balance.
X	The melt was altered from 26% KF to 20.5%, pulling rates up to 3 mm/hr. were employed.	A polycrystalline boule (#546) was grown 30 mm in diameter by 85 mm in length. The boule consisted of several grains up to 10 mm in size (Fig. 4)
XI	The 1 liter crucible and hot zone was assembled. The melt was seeded with molybdenum rod. The heat shield configuration and crucible position was similar to the standard assembly.	The thermal balance of the new hot zone was evaluated and determined satisfactory without further adjustment.

GROWTH RUN	PARAMETER VARIATIONS	EVALUATION AND RESULTS
XII	A KTb_3F_{10} seed was fabricated from boule #546 and used for this run.	Boule #550 was grown, composed of KTb_3F_{10}. Several cracks had propagated through the boule during the growth run. (Fig.6)
XIII	A clear, crack-free seed was fabricated from boule #550. The elimination of defects in the seed would reduce initiation points from which cracks could propagate into the boule.	Boule #551 was grown. This boule also cracked during the growth process. The cracking was related to cleavage tendency in KTb_3F_{10}. (Fig. 7)
XIV	The seed candidates were etched to detect grain boundaries. Only single crystal seeds were used.

Pull rates were reduced to .5 mm/hr. to reduce stress within the growing boule. | Boule #552 developed cracks similar to previous boules during the growth process. (Fig. 8) |
| XV | The melt was seeded to grow a 50 mm diameter boule. | A 53 mm diameter boule was grown to a 5 mm length. The boule was lost as the platinum wire seed support broke loose. |

eliminate crack propagation during the growth process. A
boule was grown to 53mm in diameter during growth run 15,
but subsequently lost due to failure of the platinum wire
attaching the seed to the seed rod.

3.2.1 Hot Zone Modification

The electronic nature of Tb^{+3}, with its numerous low
energy states, has a major influence on the thermal configuration
during growth. The thermally excited radiation from these
states creates a high long wavelength emissivity from the
melt and crystal. Other rare earths that we have dealt with
have either no levels, or very few levels at 5000 cm^{-1} or
less above the ground state. As a result, little radiation
from either the melt or the crystal causes little change to
the overall thermal distribution in these other systems,
while the large concentration of Tb^{+3} in KTb_3F_{10} compounds
the problem. Typical crystals grown in the past were
composed of dilute concentrations of rare earth ions, ranging
1 to 5 cation percent, whereas, KTb_3F_{10} contains 75 cation
percent Tb^{+3}.

The radiative heat loss was observed as melt instability,
leading to heterogenous nucleation and growth at the crucible
wall and on the surface of the melt. The hot zone of the
furnace has been modified through shielding redesign and
repositioning the crucible within the hot zone.

The optimized furnace configuration is presented in
Figure 3. The basic thermal transport can be described as
direct radiation heating the middle to the lower section of
the crucible, and a natural convection flow of argon through
the opening in the vertical shield, creating a vertical heat
loss. This thermal distribution will maintain the sides and
bottom of the melt hotter relative to the middle of the melt
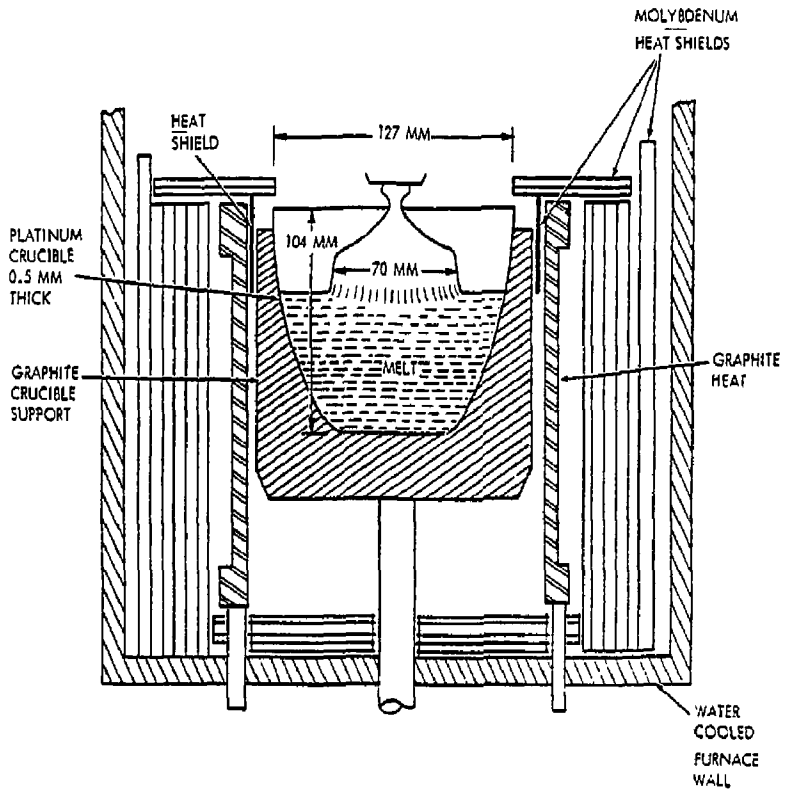surface. As a result, the seeding and growth process will

17

FIGURE 3

FURNACE ARRANGEMENT WITH ONE-LITER CRUCIBLE
FOR 7.0 cm KTb_3F_{10} CYRSTALS

occur in the coldest section of the melt, which is essential for
controlled growth. To enhance the cooling effect of the
seed rod, a 3mm diameter molybdenum "seed" was used.
The button and an early growth is shown in Figure 4.

The design of the hot zone for the one liter crucible
included modifications made to the standard hot zone as discussed
on the previous page. The crucible elevation and position was also
adopted from the earlier runs. As a result, the initial installa-
tion provided a satisfactory thermal balance as evaluated in
growth run eleven, and no modifications were necessary.

3.2.2 Melt Composition

The limited data at the beginning of the program suggested
that the melt composition should be maintained between 27% to
35% KF for proper growth conditions for KTb_3F_{10}. A proposed
peritectic reaction occurs at 26-27% KF; for compositions lower
in KF, TbF_3 is the primary phase. At a composition richer than
35% KF, precipitation of a 2nd phase readily occurred. The
first melt used in the initial growth runs contained 30 mole %
KF. The material pulled from the melt was characterized by a
hazy appearance, possible due to a 2nd phase. To avoid all
possibility of 2nd phase precipitation, we chose to
work from a melt initially close to the peritectic composition,
27% KF. The melts from growth runs six through nine were
initially composed of 26% KF. Evaporation of a potassium fluoride
rich phase from the melt complicated the "material removal -
potassium enrichment" relationship in the melt and made it
difficult to move the melt composition into the KTb_3F_{10} phase
field. The melt used for run ten, composed of 28.5% KF,
seemed to result in very adequate working composition. Over
half the melt was removed in the form of boule #546, while
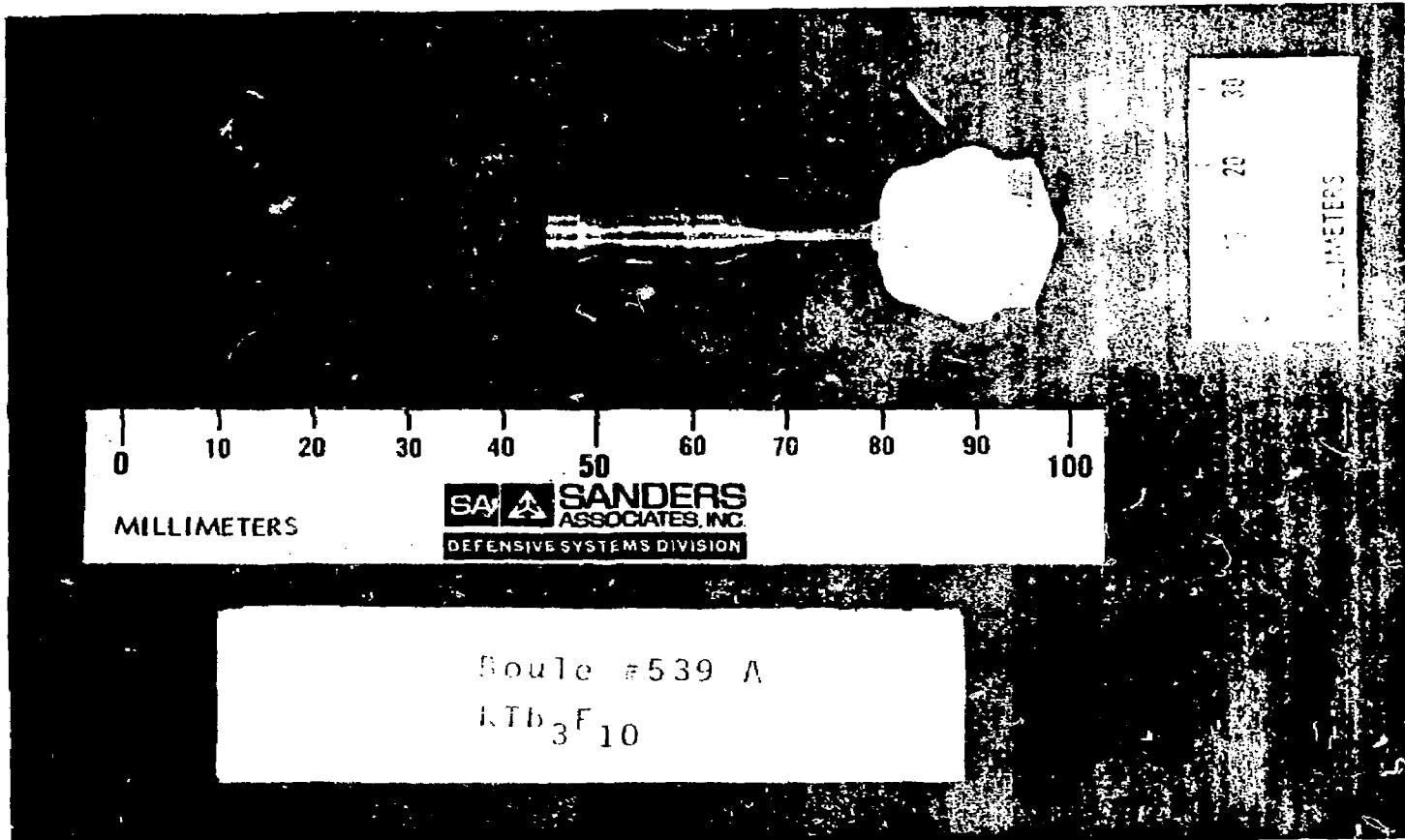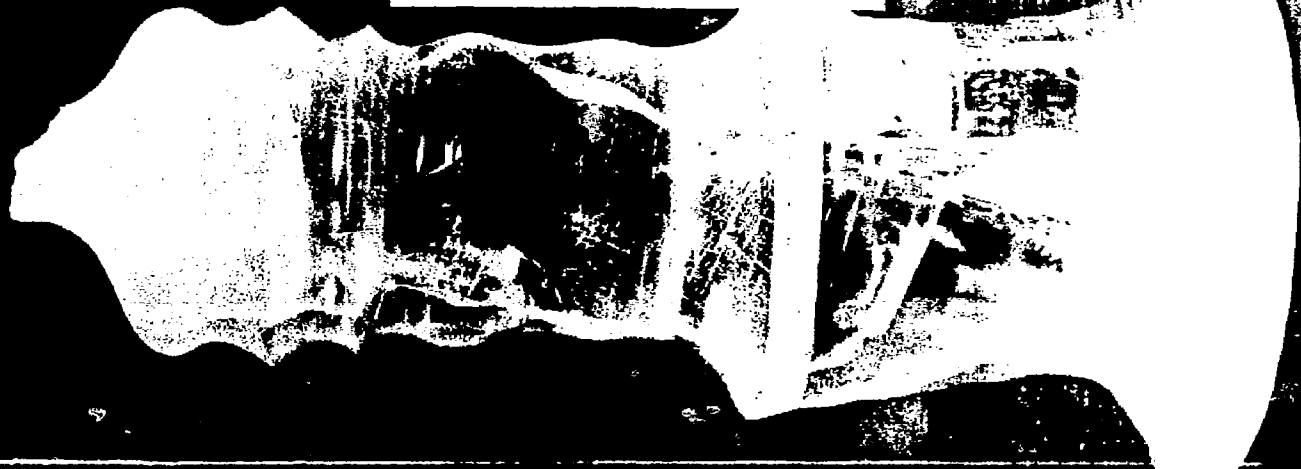only the lower section appear hazy, as shown in Figure 5.

19

FIGURE 4

Boule #546
KTb_3F_{10}

0   10   20   30   40   50   60   70   80   90

MILLIMETERS

SA SANDERS ASSOCIATES, INC.
DEFENSIVE SYSTEMS DIVISION

FIGURE 5

This indicates that at a composition of 28.5% KF, a good portion of melt may be removed without enriching the KF concentration to an unworkable level. Future melts were prepared at a 28.5% KF level.

3.2.3 Rate Parameters

The mechanical parameters affecting rate of growth are the pulling rate of the seed and corresponding rate of temperature lowering of the melt. After the seed is melted back, we use relatively high temperature lowering rates (5-10°C/hr) to approach the growth temperature of the compound. The melt instability discussed earlier limited the temperature lowering rate and thus pulling rate. Optimizing the thermal distribution of the hot zone as well as maintaining a clean melt surface improved the melt stability.

The seed pulling rates were varied considerably in run ten. A maximum rate of 3.0 mm/hr was used, but the rate of temperature lowering in the melt was much larger than desired, 6-7°C per hour. A rate of 1.5 mm/hr reduced the temperature rate of change to 3-4° hour, a satisfactory compromise.

The mechanical parameters were altered to reduce the rate of growth in later runs in an effort to prevent the cracks propagating in growing boules. If the cracks were induced by lattice stress, lower growing rates might reduce the resulting stress by allowing lattice accommodation. Seed pulling rates were reduced to .5 mm/hr in run fourteen, however, cracks still propagated in the boule.

Rotation rate of the seed rod plays a direct role upon the melt mixing and stability of the growing crystal. Increased crystal growth stability has been achieved in the past with a crystal interfacial shape convex to the melt. Slower rotation rates will alter the melt thermal distribution such that the crystal will grow convex to the melt[5]. Rotation was altered early in the program to obtain a more stable condition. Early runs indicated crystals were growing with a concave interface at a rotation rate of 30 rpm. Reduction of this rate of 6 rpm modified the interface to a flat configuration and reduced the tendency for the crystal to pull out of the melt. The rotation rate was increased slightly later in the program to enhance the mixing in the melt with little effect on the interfacial shape.

3.2.4 Seed Material

Early growth runs were "seeded" with platinum wire, later replaced with a molybdenum rod with which most of the hot zone modification was evaluated. Boule #546 was grown on the molybdenum button. The first KTb_3F_{10} seeds were cut from boule #546 and the last four growth runs were seeded with KTb_3F_{10}. Initially, limited success was obtained in producing optical quality, single crystal KTb_3F_{10}. In successive runs, as the quality of the material grown increased, the quality of the seeds increased. The seeds for runs 14 and 15 were single crystal, crack free, and absent of twin boundaries, thus reducing the possibility of crack propagation from the seed. Cracks did, however, propagate in boule #552 grown in run fourteen. The boule growing in run 15 did not contain any cracks at the time it dropped into the melt.

3.3 Evaluation of KTb$_3$F$_{10}$ Crystals

3.3.1 Boule #546

Boule #546 was nucleated on the molybdenum "seed" and grew in a roughly cylindrical shape (Figure 5). It contained numerous cracks but was optically clear except for the last to grow regions that contained a small amount of precipitate. The boule was sectioned to measure density, lattice parameters, and microstructure.

A lower section of the boule was polished and then etched in nitric acid, activated with metallic copper. The etched section, shown in Figure 6, revealed a multi-grain structure complicated by twinning. Major cracks in the crystal appear to have occurred along grain boundaries. The twin plane is apparently $\{111\}$. There were also cracks propagating along the $\{111\}$ planes related to cleavage tendencies rather than twin boundaries. Similar twins have been observed in KY$_3$F$_{10}$. Differential thermal analysis (DTA) was used to detect phase transitions in this latter material, and visual observation of the twin structure before and after cycling near the melting point, indicated that a phase transition was not responsible for the appearance of such twins .[6]

X-ray analysis and density measurements were made to determine possible compositional changes in the boule. The starting melt composition from which the boule was grown was potassium rich as related to KTb$_3$F$_{10}$. As the boule was grown, the melt was further enriched with KF as a result of crystallization of a relatively less potassium rich solid. If the solid phase consists of a solid solution of variable composition, as the melt composition becomes potassium enriched so should the solid phase. This compositional change should

MICROGRAPH OF A POLISHED SECTION FROM BOULE #546

FIGURE 6

be reflected in the lattice constant and density of the solid.
A mechanism complicating this affect, however, is a significant
evaporation of the melt which seems to be dominated by potassium
fluoride. The lattice constant, a_o, was measured on samples
from the top and bottom of the crystal, using the $\{888\}$ reflection,
as 11.671Å and 11.669 respectively. These two values agreed
within experimental error. This data indicates no noticeable
change in lattice constant during the course of the growth
run.

The x-ray density was calculated for boule #546 with a
lattice constant of 11.669Å, a formula of KTb_3F_{10} with $Z = 8$,
to be 5.901 gm/cm^3. Avagadro's number used was 6.023×10^{23}
molecules per mole. A pycnometric density was measured at the
top and bottom of the boule as 5.776 gm/cm^3 and 5.752 gm/cm^3
respectively. The discrepancy in both pycnometric values and
that of the x-ray density may be significant. The x-ray
density assumed a stoichiometric compound, which may not be
the case. If the formula is adjusted so that the calculated
x-ray density matches the measured pycnometric density, it
would be $K_{1.10}Tb_{2.91}F_{9.81}$ for the top and $K_{1.11}Tb_{2.89}F_{9.76}$ for
the bottom of boule #546. The correction assumes that
KTb_3F_{10} is a solid solution with limited substitution in the
cation sub-lattice.

The preliminary results of the x-ray analysis and density
measurements indicate that although compositional changes may
occur through the growth process of KTb_3F_{10}, there is little
if any change in the dimensions of the unit cell as a result.

3.3.2 Boules #550, #551, #552

The later KTb_3F_{10} crystals were seeded with material from
boule #546 or subsequent boules. By design, material grown in
successive runs will increase in quality. As such, the subsequent
seeds fabricated should also increase in quality.

Boules #550, 551, and 552 are illustrated in Figures 7-9, respectively. The KTb_3F_{10} crystals generally grew to a transparent appearance. The cracking occurred in the middle to later stages of the run. A small concentration of precipitate appeared in the lower section of boule #552.

The ends of boule #550 were cut and polished. The fracture pattern observed followed specific directions in the boule. Series of parallel fracture planes would cross a second set of parallel fracture planes. This crack pattern reappeared in later crystals. The major fractures again occurs along cleavage planes.

The lattice constant, a_0, was calculated from x-ray diffraction patterns for boule #550 and #551 as 11.672A and 11.666Å respectively. These values coincide with the lattice constant calculated for boule #546.

3.3.3 Optical Quality

The optical quality of the KTb_3F_{10} crystals grown at Sanders was evaluated through Twyman-Green Interferometry. Fabrication of a rectangular sample (Figure 10) 5mm x 10mm x 20mm, included grinding flat and optically polishing the ends. An interferogram, Figure 11 shows highly linearly fringes along the 20mm optical path. Through the center section wave front distortion is less than $\lambda/5$ at .633nm, minute distortion. Some edge affects are visible at the top and bottom of the sample. It is not entirely clear whether these are due to edge rounding during polishing or are intrinsic. A small crack was visible in the middle of the upper edge. Wave continuity to this degree indicates a high optical quality material, with minimal changes in the index of refraction.
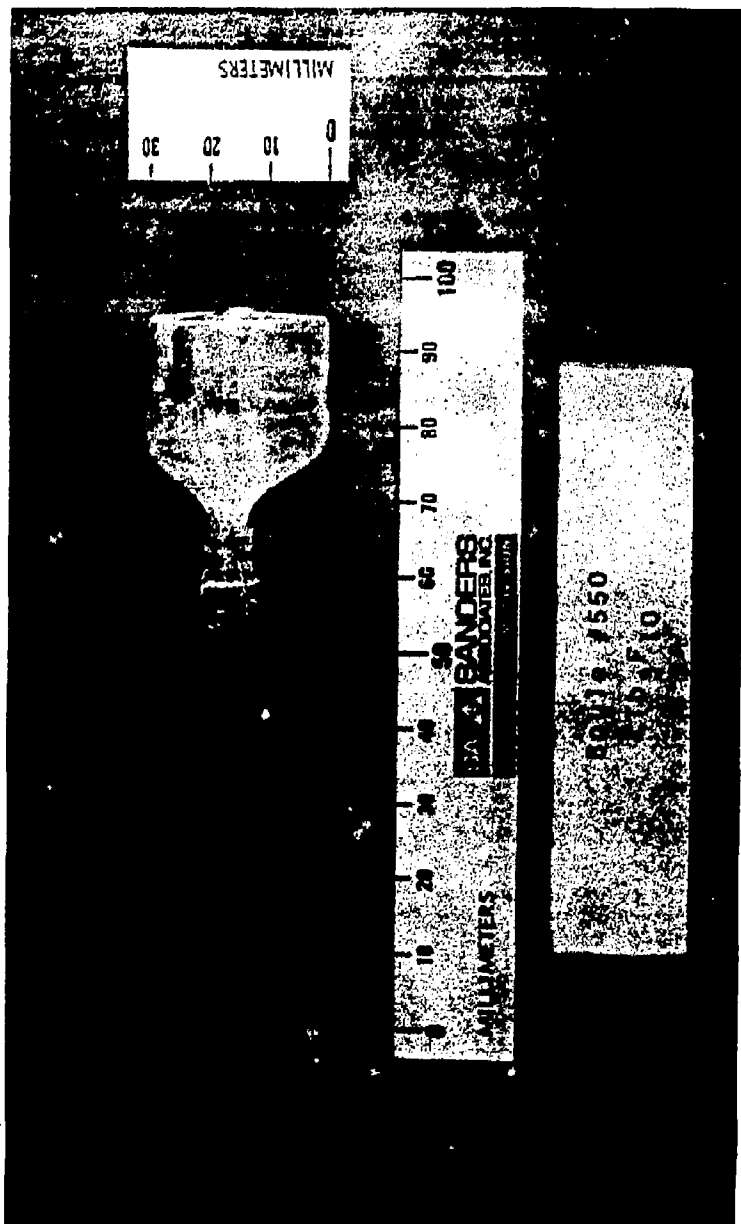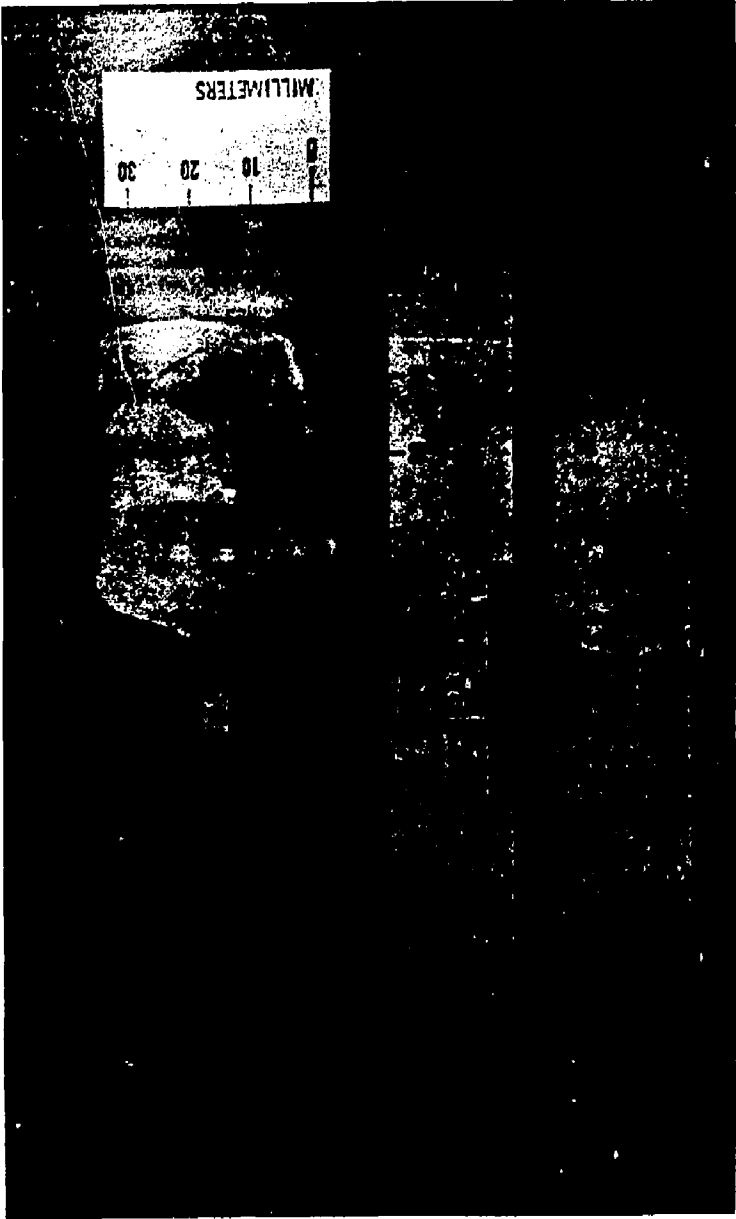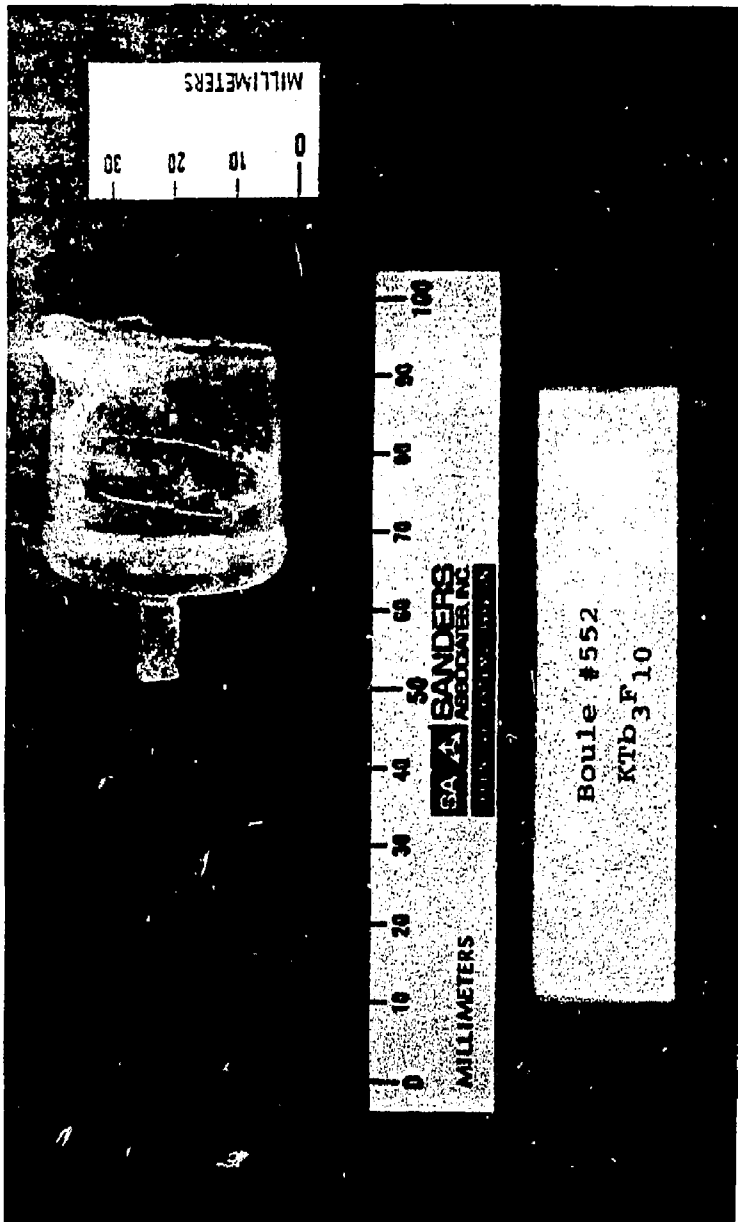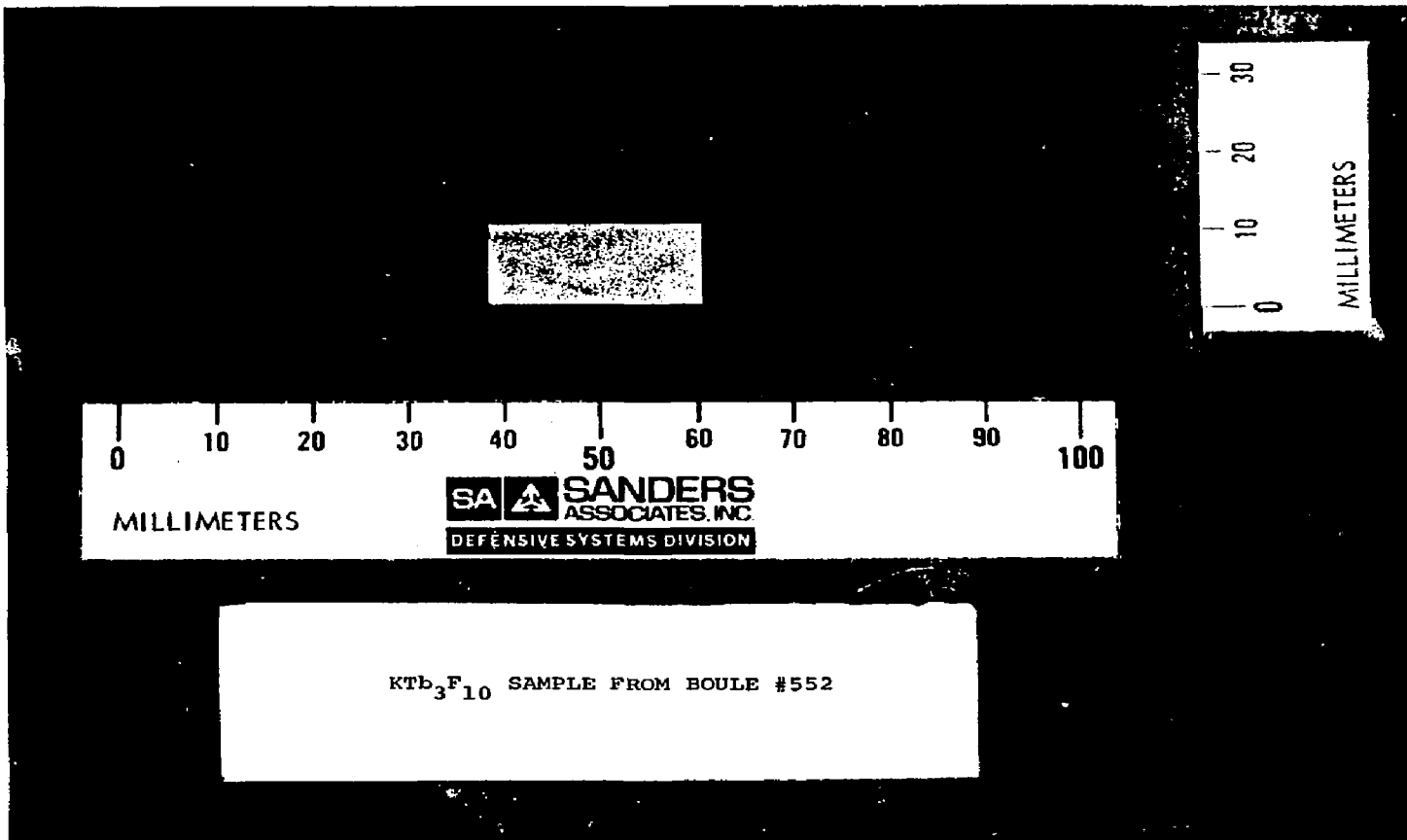
27

FIGURE 7

FIGURE 8

MILLIMETERS

Boule #552
KTb_3F_{10}

FIGURE 9

MILLIMETERS

0   10   20   30   40   50   60   70   80   90   100

MILLIMETERS

SA ▲ SANDERS
ASSOCIATES, INC.
DEFENSIVE SYSTEMS DIVISION

KTb_3F_{10} SAMPLE FROM BOULE #552

FIGURE 10

INTERFEROGRAM OF BOULE #552

FIGURE 11

4.0 DISCUSSION OF RESULTS

The growth development of a new material such as KTb_3F_{10}, requires an extensive parametric study. This task consists of furnace hot zone redesign, physical growth parameters development, and growth evaluation. The previous studies at the Crystal Physics Lab of M.I.T. has enhanced the early development, in that it produced guide-lines for hot zone design and growth parameters. The initial task in this program was to transfer these parametric guide-lines to adapt our crystal growth furnace to capacitate the growth of KTb_3F_{10}. This was performed through a series of empirical experiments and growth runs. The results of the development work has been stated in Section 3 and relate to the following: modification of hot zone for proper thermal distribution for growth of KTb_3F_{10} and successful scale in size of the hot zone; growth parameters were developed and employed successfully to growth several KTb_3F_{10} boules up to 35mm in diameter, and one boule 50mm in diameter; evaluation of boules indicated excellent optical properties of material, cleavage has limited size of boules fabricated.

4.1 Hot Zone Modification

Initial evaluation of the hot zone was performed on Sanders' standard assembly. Various techniques of shielding were evaluated to alter and adjust the thermal distribution. Early observations indicated excessive radiative energy was being emitted by the melt due to the physics of KTb_3F_{10}. As a result of this energy distribution, the melt surface behavior was unstable, e.g., turbulent flow and surface nucleation. Through the experiments, the optimum configuration developed excessive radial energy inflow and a substantial vertical loss through the top shield. Positioning the top

of the crucible at the upper edge of the heater exhanced the
thermal distribution. The melt stabilization was observed
as complete suppression of surface nucleation and growth
except at the seed interface. The major characteristics of
the standard hot zone were successfully transferred to the
larger hot zone for growth of 70mm boules. The optimal
thermal distribution was obtained through minor modifications.

4.2 Physical Growth Parameters

Physical growth parameters were also evaluated during
the early growth runs. Furnace control parameters, growth
rate, and seed rod rotation rate (mixing mechanism) all
affect the growth conditions and therefore, the quality of
the boule fabricated. Empirical evaluation was done to
develop the conditions necessary to grow KTb_3F_{10}. The maximum
growth rate employed was 1.5mm/hr, which was adequate to
grow clear, homogeneous material. The growth rate was sufficient
to counteract the change in melt composition expected due to
the evaporation process of a potassium fluoride rich phase.

The growth interface was modified by boule rotation
rate to stabilize growth processes. The interface shape
developed in early runs was concave in respect to the melt.
Under such conditions growth was unstable as loss of contact
with the melt was a common result. Reduction of boule
rotation rate, modification of melt flow, altered the interface
to a flat configuration. The melt condition was stabilized by
boule growth in this configuration.

Several KTb_3F_{10} boules were grown employing the growth
parameters developed. The quality of the growth material
improved in successive runs. The improvement in the quality
of seed material employed was primarily responsible. The
numbers of matrix defects was significantly reduced through

this refining process. The improved quality of boules was directly transferred to the seeds to be used in subsequent runs. As a result, boule #552 did not appear to contain grain boundaries and the number of twin boundaries was greatly reduced.

4.3 Evaluation of KTb_3F_{10}

4.3.1 Optical Quality

KTb_3F_{10} grown for this program appears for the most part clear. The majority of peaks for Tb^{+3} are in the infrared region. Under certain lighting conditions, a pink color tone was observed. This is related to a rare earth impurity ion, unknown at this time. The raw material, Tb_4O_7 99.9% used in this program, was not a high purity grade. Zone refining techniques are being employed to determine the nature of the impurity ion.

Two boules examined appeared to contain a section consisting of a second phase precipitate. In both cases, the precipitate was located in the lower section of the boule. These sections can be described as displaying a hazy, milky appearance.

It is suggested that the reason for the precipitate was that the boule was grown from a relatively potassium rich melt, composition approaching 35% KF. As a KTb_3F_{10} boule is grown the melt composition becomes richer in KF, and in both instances, the precipitation occurred in the lower section of the boule, the last section to grow. The occurance of the precipitate corresponds with earlier phase diagram work discussed in Section 2.0.

35

A polished sample of KTb_3F_{10} grown was examined under Twyman Green interferometry and demonstrated excellent optical uniformity. Very little distortion of the wavefront passing through the sample was observed. Variation in the index of refraction was negligible. Previous explanation of growth kinetics of KTb_3F_{10} implied that along with growth, was an associated mechanism to change the composition of the remaining melt and therefore, the future growth crystal. Although this interferometric examination is preliminary it suggests that if there is a slight composition variation in the crystal it has not affected the index of refraction of the matrix.

4.3.2 Mechanical Properties

Cleavage has been a major limitation in the size scaling of large diameter KTb_3F_{10} boules. Fracture of seeds during growth runs, which has led to the early termination of runs and the loss of two boules, seems to be related to a similar cracking mechanism as in the growing crystals. The cracks tend to propagate in definite directions in the boules and relate to cleavage directions. In the KTb_3F_{10} system, which is isometric, cleavage is on the $\{111\}$ planes. This is termed octahedral cleavage. The seed material in the previous growth runs have been orientated to grow a few degrees off the $\langle 110 \rangle$ type direction. For such an orientation, the cleavage plane was almost perpendicular to the direction of growth, and in two cases, the seed had indeed cracked perpendicular to the growth direction. It is important to identify and fix seed orientation to the optimized growth direction in this system as related to cleavage directions. The proper orientation, not yet tested, seems to be in the $\langle 100 \rangle$ directions. The cleavage planes $\{111\}$ relate to the $\langle 100 \rangle$ directions as a series of diagonal planes, such that the planes intersect to form a pyramid with $\langle 100 \rangle$ at the apex. This orientation will tend to maximize the stress required to propagate a cleavage fracture. Proper seed orientation should also reduce the cleavage tendency in the growing boules.

36

Although the mechanism for fracture of KTb_3F_{10} boules
has been identified as a cleavage mode, the driving force for
this phenomenon has not been identified. The fracture of the
seed is probably a mechanical stress caused by the weight and
motion of the rotating boule. The driving force for the
crack propagation in the boule is more complex and may be
caused by one or more of the following: stresses from thermal
gradients in the boule; inappropriate orientation; localized
differences in thermal expansion, creation of lattice stress,
and may also lead to the second phase precipitation observed
in some boules.

The x-ray diffraction analysis and pycnometric density
measurements on boule #546 suggests that although the lattice
constant, a_o, does not vary during the growth run, composition
of the boule may change to a small degree. A plausible
mechanism at work during a growth run, relating to the earlier
phase diagram (Figure 1), is that as a crystal grows, the
melt is depleted in terbium fluoride and thus the melt composition
follows the presented liquidus; the composition of the corresponding
solid phase, KTb_3F_{10}, follows the associated solidus. The
resulting crystal would be composed of a KTb_3F_{10} solid solution
enriched in potassium in the growth direction. This apparent
compositional change does not have significant effects on the
lattice constant of KTb_3F_{10} and thus it is not easily related
to the possible creation of lattice stress. It could, however,
lead to possible variations in thermal expansion which may
lead to the internal stress.

Future growth should address the possible melt compositional
change. The growth run design should consider an initial melt
composition of 27% KF (peritectic composition) and maintain
a relatively constant melt composition throughout the run.
Fabrication of a crystal as close to stoichiometric KTb_3F_{10}
will help to determine the nature of the cleavage problem,
ie., compositional dependent or an inherent property.

5.0 CONCLUSIONS

Several boules of KTb_3F_{10} were grown and determined of excellent optical quality. Crystal growth limitations occurred due to cleavage of the system. Sufficient hot forging samples were not supplied during this period. Future work to improve the crystal growth capabilities of KTb_3F_{10} include:

- Phase equilibria experiments to improve our understanding of $KF-TbF_3$ system and describe the solidification kinetics.

- Crystal growth work is presently being done in the related system of $KF-YF_3$. Detailed understanding of KY_3F_{10} will enhance future work with KTb_3F_{10}.

- Determination of proper growth orientation will enhance mechanical stability as well as improving the chemical growth process of KTb_3F_{10}.

- Investigation of hot forging KY_3F_{10} and at a later date KTb_3F_{10} should be done.

REFERENCES

1. N.F. Borelli, J. Chem, Phys-41, 3289 (1964).

2. M.J. Weber, et. al, J. Applied Physics (49) 6.

3. David Gabbe, Massachusetts Institute of Technology, (private communication) June 1978.

4. R.C. Folweiler, et al., High Power Laser and Material Investigation, Report #2, Contract D.E.-AC08-78-DP40054. Department of Energy, 1978.

5. J.R. Carruthers J. of Crystal Growth 36 (1976).

6. J. Pierce, Lincoln Laboratory (private communication).